SciEn Proceedings of 8th International Conference on Mechanical, Industrial and Energy Engineering 2024
02-04 January, 2025, Khulna, BANGLADESH
SciEn Conference Series: Engineering Vol. 3, 2025, pp 411-414 https://doi.org/10.38032/scse.2025.3.111

Aerodynamic Performance Analysis of a Dual-Purpose Aircraft for Targeted Payload Delivery

M A Wadud[1], Mohammad Nahidul Islam[2], Md Arifuzzaman[1] and Md Shariful Islam[1]*

[1]Department of Mechanical Engineering, Khulna University of Engineering & Technology, Khulna-9203, Bangladesh
[2]Department of Chemical Engineering, Khulna University of Engineering & Technology, Khulna-9203, Bangladesh

ABSTRACT
The landscape of modern delivery services is changing due to the convergence of technological innovation and changing customer behavior. In response to the increasing e-commerce demands and the issues created by urban congestion and environmental concerns, this study provides a conceptual design and simulation for an autonomous aerial vehicle customized to the complexities of modern logistics. This research examines the possibility of airborne delivery technologies to change last-mile delivery. With established delivery businesses and merchants delving into airborne distribution, the potential of using planes to avoid traffic congestion and cut carbon emissions is becoming more apparent. The center of this project is developing a customizable airborne vehicle capable of direct point-to-point delivery, reducing delays and human interaction. The paper must overcome several limitations, such as a maximum Thrust-to-Weight ratio of 0.75, a compact wingspan of less than 120 cm, and the capacity to function from semi-prepared surfaces. The aerodynamic performance of the NACA 0009 airfoil was analyzed using xlfr5 software. The maximum drag and lift coefficient was found at 10° and 8° respectively. The neutral point is located above the center of gravity of the aircraft which ensures the stability of the aircraft.

Keywords: Aerodynamics, Payload Delivery, Short Takeoff and Landing, xlfr5

1. Introduction

Every airplane relies mostly on the geometry of its wings. The creation of lift results from the rapid sweeping of a wing through the air. They may be made into several shapes. The balance and stability of the wing, the amount of lift it generates, and how easily it can be maneuvered at different speeds are all affected by its shape. The leading and trailing margins of the wing might be straight or curved, or they can be different shapes altogether [1]. Both the leading and trailing edges of the wing may be tapered, with the former producing a leading edge that is narrower than the root (where it connects to the fuselage) [2, 3].

The landscape of delivery services is undergoing a revolutionary transformation in a world driven by technological breakthroughs and shifting customer needs. This study goes into the world of airborne delivery systems, providing a conceptual design aimed at tackling modern-day logistical difficulties. As e-commerce grows and urban congestion worsens, the demand for creative, efficient, and sustainable delivery options becomes more pressing [4].

The development of an adaptive airborne vehicle capable of last-mile delivery with efficiency and precision is key to this goal. The capacity of aerial vehicles to create direct links between source and destination, avoiding delays and human involvement, gives them a distinct advantage. This research investigates the practicality of such a vehicle in addressing the difficulties of modern delivery issues [5, 6].

Unmanned Aerial Vehicle (UAV) systems have become increasingly important in both military and civilian operations due to their diverse capabilities and the evolving needs of various industries. The development and deployment of UAVs require a multidisciplinary approach, as these systems integrate principles from several engineering fields, including aerodynamics, electronics, materials science, and structural engineering. The systems nature of UAVs involves harmonizing these disciplines to achieve optimal performance and fulfill specific operational requirements, which often differ significantly from those of manned aircraft. One of the key distinctions between UAVs and manned aircraft lies in their unique design considerations and functional objectives. UAVs are typically designed to operate without an onboard human pilot, which allows for different design constraints, such as reduced need for life-support systems, smaller structural components, and increased flexibility in weight distribution. The autonomy and control aspects of UAVs also necessitate the integration of advanced electronics and software systems, which can handle tasks such as navigation, communication, and real-time decision-making. These differences have a profound impact on the design, testing, and deployment phases, with UAV systems often requiring specialized approaches to address the unique challenges posed by remote operation, such as signal latency, autonomous decision-making, and varying environmental conditions [5, 7].

This paper begins a design study, utilizing the xlfr5 program to create basic designs that serve as the foundation for the proposed aerial vehicle. Considerations of bending moments,

*Corresponding Author Email Address: msislam@me.kuet.ac.bd
Published By: SciEn Publishing Group

lift-to-drag coefficients based on angle of attack, neutral points, wing areas, and the delicate interaction of stability coefficients are all integral to this process. This work attempts to achieve a compromise between performance and dependability by assessing and adjusting the aircraft's dynamic stability. The design selections are supported by the contest's specified thrust-to-weight ratio, which directs attention to a Short Takeoff and Landing (STOL) configuration that matches the design criteria [8, 9].

2. Methodology

The attainment of wing stability in the primary design is a prerequisite for conducting Computational Fluid Dynamics (CFD) simulations. Before proceeding, it's imperative to ascertain the acceptability of the force outcomes derived from the fluid simulation. Hence, validation of the simulation procedure becomes essential. In this context, a similar study focusing on wing drag and lift coefficients is referenced for validation, using the NACA 2412 airfoil. Subsequently, the validated setup will be applied to simulate the preliminary design.

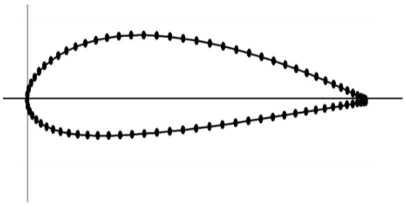

Fig.1 Schematic diagram of NACA 2412.

For the CFD simulation within this project, xlfr5 software was employed, utilizing the Fluent Solver. As depicted in Figure 1, the NACA 2412 airfoil was generated, and the simulation was executed on a 3D model of the NACA 2412 airfoil at a Reynolds number of 200,000. The selection of the Reynolds number was guided by reference sources, serving the purpose of validation [10].

The entire process was carried out systematically using the xlfr5 software, following a step-by-step approach. This section outlines the comprehensive procedure for generating the model and conducting subsequent analyses to assess its viability. For the aircraft shown in Figure 2 (a) and (b), the NACA 0009 airfoil was chosen to shape the wing, elevator, and fin. Initially, the software's direct foil analysis feature was utilized to develop the airfoil model. The NACA 0009 airfoil boasts specific characteristics and dimensions. This airfoil was selected as the foundational design and to control the aircraft's rolling and pitch maneuvers. To effectively manage these movements, both flaps and ailerons were implemented. Notably, flaps set at angles of +7 degrees (downward) and -7 degrees (upward) were incorporated along the trailing and leading edges. Reynolds number was chosen from 20,000 for the analysis. The range chosen for the angle of attack was from -7 degrees to 10 degrees with an increment of 0.5 degrees. The forced transition for both top and bottom locations was set at 1.00. After that, the analysis was run, and the results were successful. After the initial development of airfoils, it is necessary to do some 2D analysis for different Reynolds numbers and other factors. So, a multi-threaded batch analysis was done on these airfoils. Other airfoils were also tested for further analyses while alternative airfoils underwent scrutiny, it was observed that the NACA 0009 airfoil yielded the most favorable outcomes in terms of lift, drag, and overall stability.

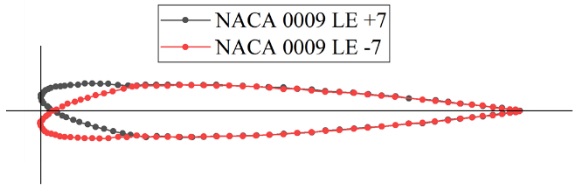

(a)

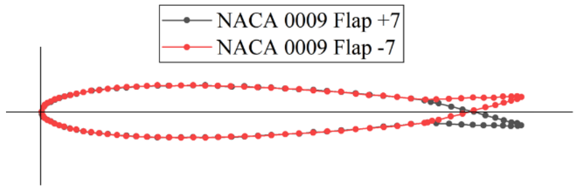

(b)

Fig. 2. (a) NACA 0009 flap at leading edge (b) NACA 0009 flap at leading edge. Both +7 and -7 degrees.

In Figure 3 (a), the primary aircraft wing had a 120 cm wingspan, a projected span of 118.18 cm, and an 18.00 cm mean geometric chord where the root chord and tip chord were 20 cm and 16 cm. The aspect ratio and taper ratio were given at 6.67 and 1.25 respectively and the root-to-tip sweep was 8.53 degrees. A 10-degree dihedral angle boosted lift and landing clearance while meshing employed a cosine distribution.

At the aircraft's tail, the elevator-controlled pitch using a 37.4 cm wingspan, a 4.89 cm mean aerodynamic chord where the root chord and tip chord were 6 cm and 3.36 cm, and an adjustable end flap for altering nose elevation. The aspect ratio and taper ratio were given 7.64 and 1.65 respectively and the root-to-tip sweep was 4.31 degrees. The 16 cm wingspan long fins featured a rudder, similar to the wing and elevator, to manage yaw. The root chord and tip chord were 6 cm and 5 cm. The aspect ratio and taper ratio were given at 2.91 and 1.20 respectively and the root-to-tip sweep was 8.53 degrees. This fin's precise design and placement were crucial for stability, adhering to demanding safety and performance standards.

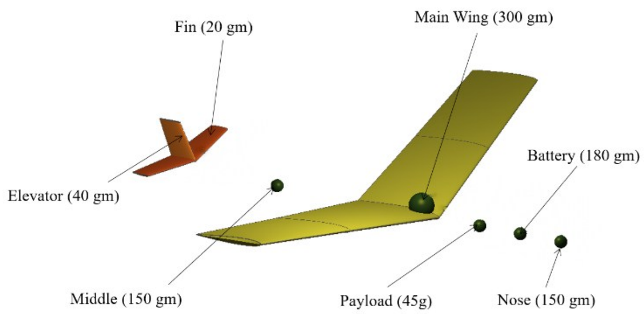

Fig. 3. (a) The xlfr5 aircraft wing model (b) Mass allocation and distribution of the whole aircraft.

The weight distribution was the major issue while designing any aircraft. We assumed that the aircraft should carry one or more than one payload (weight - 45g, diameter - 43mm). Since we will be using battery-operated aircraft with no need for fuel, the weight during the cruise of the aircraft is also going to remain constant. Weight remains constant with constant altitude at cruise. So, the maximum weight will be at the cruise position. Since we assumed the maximum thrust-to-weight ratio should be 0.75, so this was an important aspect to keep in mind.

First, we need to determine the empty aircraft weight,
W_{empty} = wing + fuselage + fin + elevator + additional mass
So, W_{empty} = 300 + 270 + 20 + 40 + 180 = 810 gm
Total weight is $W_{total} = W_{empty} + W_{payload}$ = 810 +45 = 855 gm =0.855 kg or 0.855*9.81 N = 8.4 N
Now, T/W=0.75
So, T=0.75*8.4 = 6.3 N
Thrust = Mass flow rate * Velocity
Velocity = (Re * kinematic viscosity)/ chord length = (20000 * $1.51*10^{-5}$)/0.18 = 1.675 m/s
So, Mass flow rate =Thrust/Velocity = 6.3 / 1.675 = 3.76 kg/s

Finding the proper position of every component inside and outside of the aircraft is necessary for the proper climb, cruise, descent, and overall control of the aircraft. Based on this the center of gravity will change, the location of which is vital for the stability of the aircraft. In Figure 3 (b), the weight distribution of the aircraft's different components is described. The front part, or nose, had a mass of 150 gm and was situated 30 cm ahead of the zero-coordinate point. The battery's weight was 180 gm, the payload's weight was 45 gm, and the section between the wing and tail weighed 120 gm. These mass assignments were carefully selected to achieve proper balance and maintain favorable weight-to-thrust ratios. While adjustments to the mass distribution can yield satisfactory results, excessive modifications may jeopardize the aircraft's longitudinal and lateral stability.

For stability performance at first, the analysis needed to be defined and made. Fixed lift type 2 analysis was chosen for the analysis and the Ring vortex VLM2 method (Vortex Lattice Method) was selected with viscous properties. For inertia, the previously defined mass properties were chosen, and other options were left unchanged.

3. Results and Discussion

Jacobs et al., [10] present the results of an investigation into the aerodynamic characteristics of 78 related airfoil sections. The tests were conducted in the NACA variable-density wind tunnel at a large value of the Reynolds number. The variation of the aerodynamic characteristics with variations in thickness and mean-line form were systematically studied. A wide range of airfoil geometries were tested in a wind tunnel under different airspeeds and angles of attack. The lift, drag, and pitching moment of each airfoil section were measured. In addition, the points where laminar flow transitioned to turbulent flow were identified, which helped to improve our understanding of boundary layer phenomena.

The validation process involved comparing experimental data and simulated results for the coefficient of drag (Cd) and coefficient of lift (Cl) of the NACA 2412 airfoil at different angles of attack. Figures 4 (a) and (b) illustrated that The comparison between experimental and simulated values reveals a consistent correspondence across the entire range of angles of attack. Notably, the deviations between the experimental and simulated values remain within an acceptable margin. This agreement underscores the accuracy and dependability of the simulation approach employed in xlfr5.

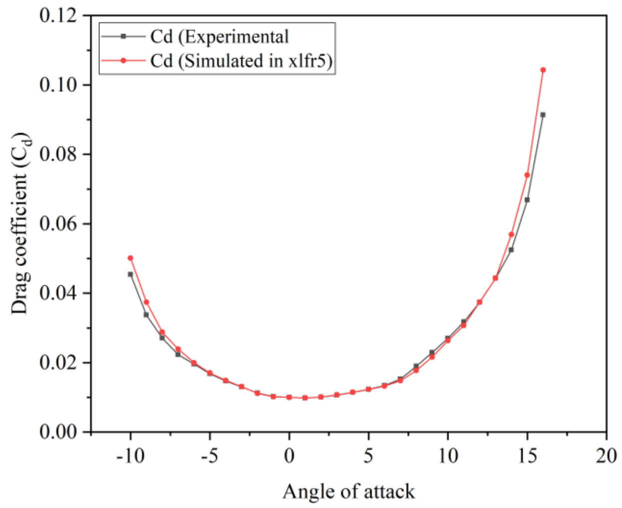

(a)

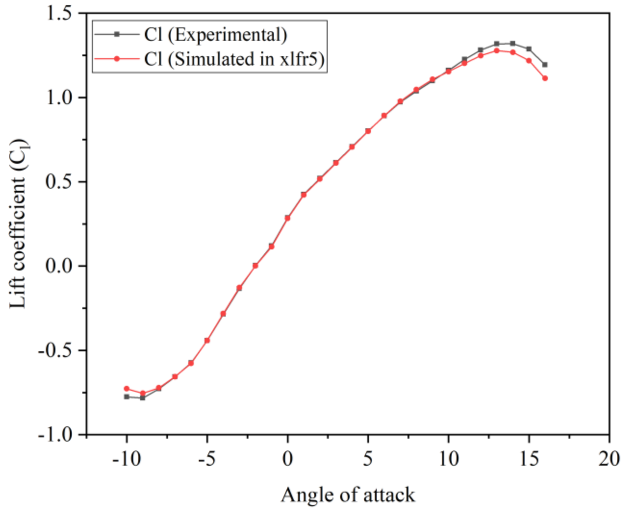

(b)

Fig. 4. (a) Angle of attack vs drag coefficient for validation (b) Angle of attack vs lift coefficient for validation.

The thorough 2D airfoil study of the NACA 0009 model, which serves as the foundation for all aircraft components, provided useful insights. We discovered a direct link between the Reynolds number and both lift and drag coefficients using multi-thread batch analysis, suggesting the importance of flow conditions on aerodynamic performance. Furthermore, in Figure 5 (a) and (b) the analysis of lift characteristics at different angles of attack revealed comparable tendencies. The lift coefficient (Cl) rose as the angle of attack increased, demonstrating the underlying aerodynamic tendency. Intriguingly, drag coefficient (Cd) patterns revealed a differential between positive and negative angles of attack. Cd fell at negative angles of attack before continuing an increasing trend for positive angles of attack, highlighting the complex interaction of forces. These findings support the applicability of the NACA 0009 model for the design, which is consistent with our goal of developing an efficient and stable aerial vehicle.

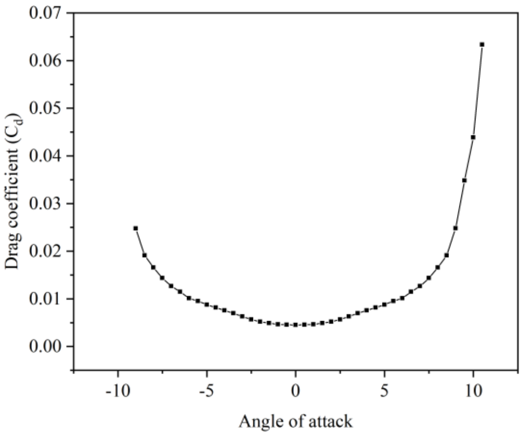

(a)

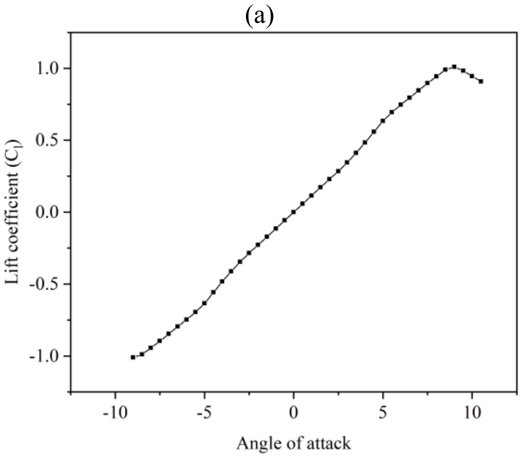

(b)

Fig. 5. (a) Angle of attack vs drag coefficient for NACA 0009 (b) Angle of attack vs lift coefficient for NACA 0009

From Figure 6 (a) we see that for negative AOA we have a positive pitching moment and for positive AOA we see a negative pitching moment. Zero pitching moment occurs at about 0.3 degrees AOA. For these, the plane will have longitudinal stability.

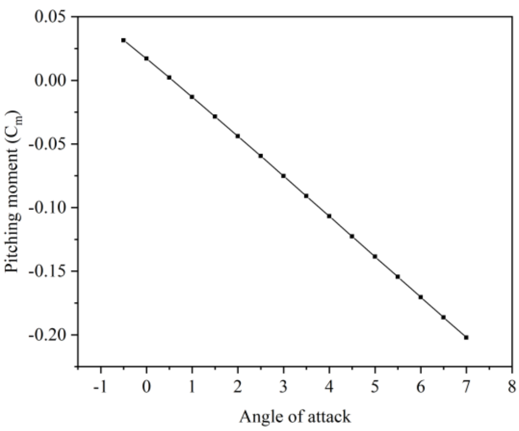

Fig. 6 (a) Angle of attack vs drag coefficient for NACA 0009

Figure 6 (b) illustrates the neutral point in the xlfr5 graph denotes the point where the aerodynamic center (AC) and the center of gravity (CG) coincide. As shown in the figure, the neutral point is located at 11.43 cm, while the CG is at 4.351 cm, which results in an aerodynamic chord of 18.074 cm. The static margin, which is the distance between the neutral point and the CG, is about 0.4, indicating a positive value and thus, high stability of the aircraft.

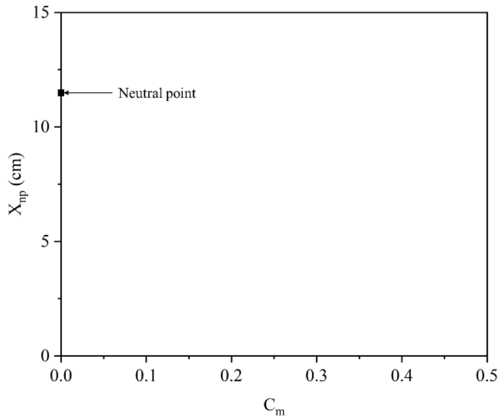

Fig. 6 (b) Angle of attack vs lift coefficient for NACA 0009

5. Conclusion

The aerodynamic performance of a dual-purpose aircraft was analyzed and optimized using xlfr5 software. The following points highlight the summary of the findings-

The project embarked on designing an autonomous aerial vehicle to revolutionize current delivery services, focusing on efficient last-mile delivery solutions.

I. The coefficient of drag for NACA 0009 airfoil was found maximum at an angle of attack of 10° while the maximum coefficient of lift was found at 8° angle of attack.

II. The pitching moment decreases with increasing angle of attack.

III. The neutral point was found at 11.43 cm at 0 pitching moment which is located above the center of gravity (4.351 cm) indicating the stability of the aircraft.

References

[1] Aziz, M.A.B. and Islam, M.S., 2017. Effect of lower surface modification on aerodynamic characteristics of an airfoil. In International Conference on Mechanical Engineering and Renewable Energy.

[2] Sadraey, M.H., 2024. *Aircraft design: A systems engineering approach*. John Wiley & Sons.

[3] Diekmann, J.H., 2019. Flight mechanical challenges of STOL aircraft using active high lift. J*ournal of Aircraft*, 56(5), pp.1753-1764.

[4] Smith Jr, K.R. and Belina, F.W., 1974. *Small V/STOL aircraft analysis*, volume 1 (No. NASA-CR-2425). NASA.

[5] Austin, R., 2011. *Unmanned aircraft systems: UAVs design, development and deployment*. John Wiley & Sons.

[6] Heintz, C., 2001. Anatomy of Stol Aircraft: Designing a Modern Short Take-off and Landing Aircraft.

[7] Howe, D. and Ward, R.E., 1972. Airplane design study STOL airliner (A71). Part 1-configuration description and data.

[8] Vural, M. and Nicolai, L.M., 2009. Estimating R/C model aerodynamics and performance. *Illinois Institute of Technology*.

[9] Güzelbey, İ.H., Eraslan, Y. and Doğru, M.H., 2018. Numerical investigation of different airfoils at low Reynolds number in terms of aerodynamic performance of sailplanes by using XFLR5. *Karadeniz Fen Bilimleri Dergisi*, *8*(1), pp.47-65.

[10] Jacobs, E.N., Ward, K.E. and Pinkerton, R.M., 1933. *The Characteristics of 78 related airfoil sections from tests in the Variable-Density Wind Tunnel* (No. 460). US Government Printing Office.